Neuropsychobiology 17: 85–99 (1987)

0302–282X/87/0172–0085$2.75/0

Spectral Analysis of the EEG

Some Fundamentals Revisited and Some Open Problems

G. Dumermuth, L. Molinari

Children's University Hospital, Zurich, Switzerland

Key Words. Spontaneous EEG activity · Frequency analysis · Time series · Postprocessing of the EEG

Abstract. This tutorial was presented during the 1986 training course of the International Pharmaco-EEG Group (IPEG) in Santa Margherita Ligure, Italy. During recent years spectral analysis has been increasingly used in experimental EEG. However, to avoid misinterpretations of results, its limitations must still be carefully considered. The tutorial starts with revisiting the fundamentals of the technique, emphasizes the practical estimation of auto- and cross-spectra, discusses the assumptions underlying the spectral analysis of stochastic processes, and ends with a brief discussion concerning the postprocessing of spectral data.

Categories of EEG Activities

When working in the frequency domain, it is useful to divide EEG activities into three different categories: (1) spontaneous nonparoxysmal or background activity; (2) spontaneous paroxysmal activity, and (3) activity evoked by external sensory stimulation.

The basic linear transformation system used in spectral analysis is that of the trigonometric functions. Each coefficient resulting from the Fourier transformation represents the average product of an epoch of EEG data with a sine or cosine wave of the same length at a specified frequency. Consequently, it is quite obvious that in the frequency domain representation rhythmic components are relatively enhanced at the corresponding frequencies, whereas transients, as e.g. spikes, are smeared over the spectrum and, therefore, no longer recognizable. From this it follows that the principal field of spectral analysis is *background activity*, whereas in the other two categories there exist only special cases to which standard spectral analysis can be successfully applied.

Paroxysmal activity is not generally suited for spectral analysis, as the variance of the transients is smeared over the spectrum, and detailed information is lost. However, its presence may show up within spectral sequences by e.g. (1) transient power increase; (2) broadband spectral changes, and/or (3) spectral ripples.

Some Fundamentals

Random Processes

Like many other biophysical phenomena the EEG shows more or less irregular patterns and can be described by average properties only. Obviously, the EEG records belong to the category of random data which cannot conveniently be described by explicit mathematical relations, but are described in statistical terms, i.e. by probability distributions and averages such as means, variances, covariances and spectra, higher order moments, etc.

The analytical approach is to define a random process x(t) generating 'realizations' which may be thought of as random functions, having statistical features as close as possible to the observed data. A random (or stochastic) process represents the collection of all possible sample functions which the random phenomenon might have produced. Such a collection is called an ensemble. Hence

a sample record of EEG data may be regarded as one single realization of a random process. In this setting the formulation of hypotheses and their statistical testing first becomes possible on a sound basis. However, it must be kept in mind that a random process is a mathematical abstraction rather than a physical reality.

Statistical Description of a Random Process

The *autocovariance* of a zero mean stationary random signal x(t) sampled at equally spaced intervals of length Δt is defined by

$$C_{xx}(k\Delta t) = E\{x(n\Delta t)x[(n+k)\Delta t]\}, \quad (1)$$

stationarity implying that the right side depends on k only.

For k = 0 we get

$$C_{xx}(0) = E[x(n\Delta t)^2], \quad (2)$$

i.e. the variance of the signal. The standardized autocovariance

$$R_{xx}(k\Delta t) = C_{xx}(k\Delta t)/C_{xx}(0) \quad (3)$$

is called the *autocorrelation* function and, being scale independent, is more often used for illustration purposes. The *cross-covariance* between two stationary time series x(t) and y(t) (with zero means) is defined as

$$C_{xy}(k\Delta t) = E\{x(n\Delta t)y[(n+k)\Delta t]\}. \quad (4)$$

Before the advent of the fast Fourier transform, an important role of the covariance functions was as an intermediate step toward spectral analysis. The *power spectrum (autospectrum, variance spectrum, spectral density)* can be most simply defined as the Fourier transform of the autocovariance function. Its usefulness is, however, to be seen in its interpretation: in fact, every stationary stochastic process can be approximated to any precision by a sum of uncorrelated sinusoidal waves with random amplitudes and phases whose average power is given by the spectral density at the corresponding frequency. This can be stated in exact mathematical terms using the *Cramèr* or *spectral representation* of stationary processes which gives the theoretical basis for the estimation of the spectral density based on the Fourier transform of the data. In the case of a real discrete time series, the spectral density is defined by

$$S_{xx}(f) = \Delta t \sum_{-\infty}^{\infty} C_{xx}(k\Delta t) \exp(-2\pi i f k \Delta t), \quad (5)$$

provided that the series on the right side converges absolutely. The *cross-spectrum* $S_{xy}(f)$ forms a Fourier transform pair with the cross-covariance function and is a complex valued function composed of the cross-spectral amplitude $|S_{xy}(f)|$ expressing the average intensity of activity shared by two time series as a function of frequency and the phase angle

$$\arg[S_{xy}(f)] = \arctan[\mathrm{Im}\, S_{xy}(f)/\mathrm{Re}\, S_{xy}(f)] \quad (6)$$

(where Im z and Re z denote the imaginary and the real part of the complex number z; arctan = $\tan^{-1}$) expressing the average phase difference between their common frequency components. The *coherence* spectrum is derived from the cross-spectral amplitude and the two corresponding power spectra,

$$\gamma(f)^2 = |S_{xy}(f)|^2/[S_{xx}(f)S_{yy}(f)], \quad (7)$$

and gives a measure of the squared correlation between two time series for each frequency component. Its values are always between 0 and 1.

Practical Estimation of Auto- and Cross-Spectra

A good estimation procedure for auto- and cross-spectral densities, including coherences, involves several steps, each step requiring the use of carefully chosen techniques. This is particularly true when the expected range of these spectra varies over several orders of magnitude, and the computations are carried out in an automatic fashion.

Effects from Digitizing, Aliasing

Modern analytical techniques are performed on a digital computer. Therefore, the effects of digitizing the data, i.e. of sampling a continuously defined series at equidistant points on the time axis, have to be considered more closely. It can be shown that the highest frequency which can be recognized by equally spaced sampling corresponds to $f_{Ny} = 1/(2\Delta t)$, where Δt is the sampling interval and f_{Ny} is called the *Nyquist* frequency. Frequency components higher than f_{Ny} are not only improperly recognized, but are even misinterpreted as lower frequencies. This effect is generally known as *'aliasing'*.

It must be emphasized that there exists no procedure to compensate this effect after sampling. Therefore, frequencies higher than f_{Ny} must be removed before digitizing by analog low-pass filtering, or else f_{Ny} has to be cho-

sen at a value higher than the highest frequency actually present (whether of interest or not!). To perform the digital calculations most economically, the high-frequency part which is not of interest for analysis should, therefore, be removed before digitizing.

Problems of Leakage and Stability

The basic estimate of the spectral density is given by the raw *periodogram:*

$$I_{xx}(f) = N\Delta t/C \left| 1/N \sum_{n=0}^{N-1} u(n+0.5)/N\, x[n] \exp(-2\pi i f n \Delta t) \right|^2 \quad (8)$$

$$= N\Delta t/C \left| \sum_{k=0}^{N-1} X(f-k\Delta f)\, U(k\Delta f/\Delta t) \right|^2$$

with $0 < f \leq f_{Ny}$, $\Delta f = 1/(N\Delta t)$, x[0],..., x[N−1] equally spaced sampled values from a stationary process, u(x), with u(x) = 0 for $x < 0$ and $x > 1$, a *data window* or *taper,*

$$X(f) = 1/N \sum_{n=0}^{N-1} x[n] \exp(-2\pi i f n \Delta t), \quad (9)$$

the Fourier transform of the data,

$$U(f) = 1/N \sum_{n=0}^{N-1} u(n+0.5)/N \exp(-2\pi i f n \Delta t), \quad (10)$$

the Fourier transform of the taper, called the *frequency window,* and

$$C = 1/N \sum_{n=0}^{N-1} u(n+0.5)/N^2 = N\Delta t \int_{-f_{Ny}}^{f_{Ny}} |U(f)|^2\, df. \quad (11)$$

The simplest data window is the *rectangular* or *Dirichlet* taper, u(x) = 1 for $0 < x < 1$, which corresponds to the unmodified raw data. Notice that in practice the periodogram is calculated only at the so-called Fourier frequencies $f_k = k\Delta f$, k = 1,..., N−1.

Expectation and Leakage

If x [n], n = 0,..., N−1 are equally spaced observations (amplitudes) from a zero mean stationary time series with spectral density S_{xx} (f), then the expected value of the periodogram is given by

$$E[I_{xx}(f)] = N\Delta t/C \int_{-f_{Ny}}^{f_{Ny}} |U(a)|^2\, S_{xx}(f-a)da. \quad (12)$$

Note that equation (12) holds for nonzero mean processes also, provided that f is a Fourier frequency. For well-chosen tapers the function U is concentrated around 0, and the expected value of the periodogram is a weighted average of the whole spectrum S_{xx} with weights concentrated in a neighborhood of f.

The periodogram is exactly unbiased for S_{xx} (f), for all f, only when S_{xx} is a constant; if this is not the case, there is *'leakage'* from all frequencies into I_{xx} (f), i.e. the whole spectral density, and especially high peaks nearby f contribute to the expectation of I_{xx} (f) which is, therefore, systematically distorted.

The function $1/C|U(f)|^2$ for the *cosine* taper – also called *hanning,* $u(x) = 0.5 \cdot [1-\cos(2\pi x)]$ – is represented in figure 1, together with the envelope of the Dirichlet taper. The form of this curve with its side lobes, which determine the behavior of the estimate in the neighborhood of a sharp peak of S_{xx}, is typical for all tapers. The higher the side lobes the more important the possible bias of the estimate, and in this respect the Dirichlet taper is particularly ill-behaved. Other aspects of the frequency window may be of relevance (e.g. width of the main lobe or distance of the side lobes from the main lobe), and a variety of tapers and of figures of merit to compare them have been developed over the years [Harris, 1978]. Among all windows we recall the *partial cosine* taper proposed by Tukey which has been successfully used for a long time and is defined by:

$$u(x) = \begin{cases} 0.5 \cdot [1 - \cos(\pi x/d)] & 0 \leq x < d \\ 1 & d \leq x \leq 1-d \\ 0.5 \cdot \{1 - \cos[\pi(1-x)/d]\} & 1-d < x \leq 1 \end{cases} \quad (13)$$

for some d between 0 and 0.5. This taper gives a decently rapid decrease of the side lobes without loosing too much information. The *prolate spheroidal* taper of Thomson [1977] practically eliminates the side lobes, making the possible bias in the estimate of a pure local nature. Figure 2 represents the function $1/C|U(f)|^2$ for these two tapers.

Remark: as indicated by equation 8, the taper can be equivalently applied in the time or in the frequency domain. In this latter case the bias-reducing properties of the taper are preserved only if the convolution is applied to the complex Fourier transform, i.e. before squaring it to give the periodogram [Bingham et al., 1967; Van Schooneveld and Frijling, 1981].

Variance and Covariances

The periodogram is not a statistically consistent estimate, i.e. its sampling error does not tend to zero when the amount of available data increases, and, moreover, due to the approximate statistical independence of the individual estimates, the periodogram has usually a very wild appearence, making the study of the fine structure

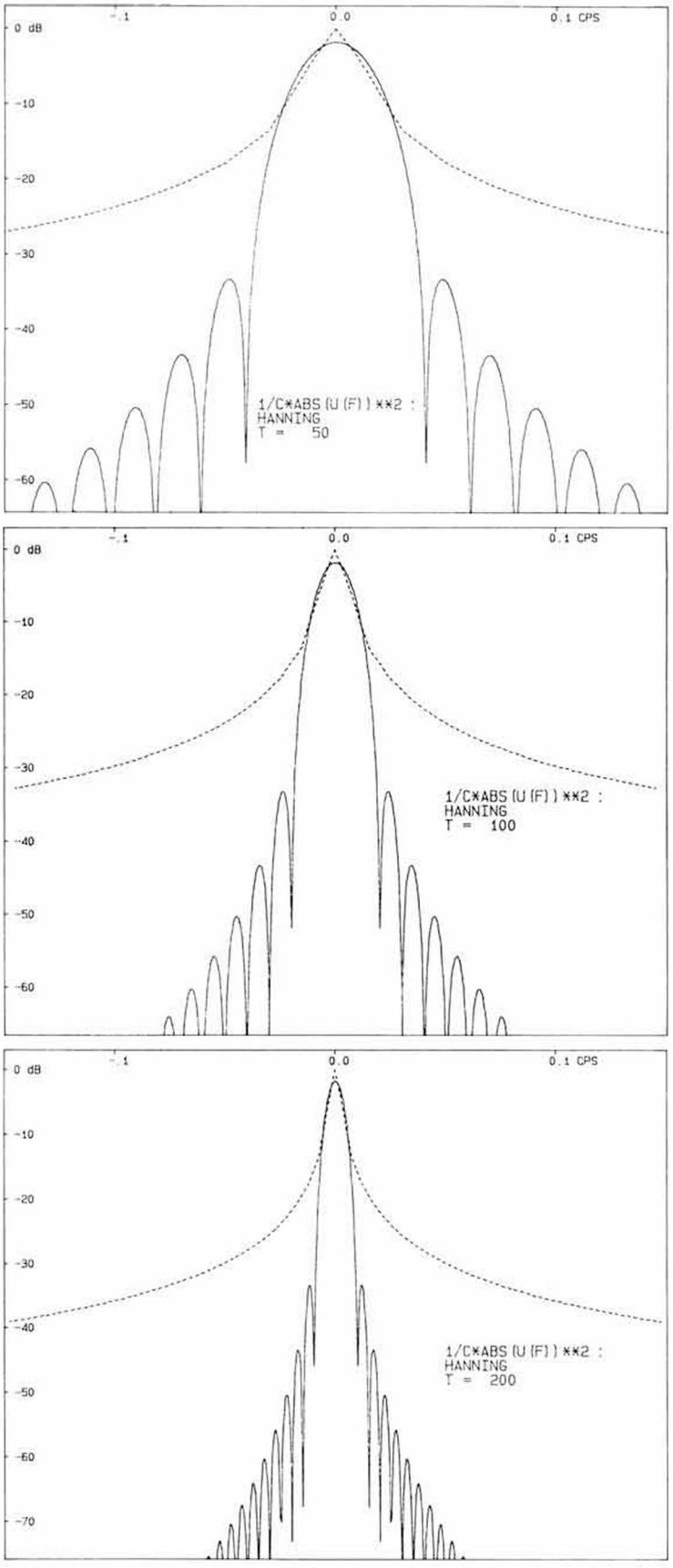

Fig. 1. Squared frequency window of the cosine taper (hanning) and envelope of side lobes of the rectangular (Dirichlet) taper for different recording lengths T = 50, 100, and 200 ($\Delta t = 1$). This shows that the danger of substantial leakage is still high for series of larger size (T = 200) if no taper is used. This must be kept in mind in the case of estimating power spectra by averaging short sections (Welch's method).

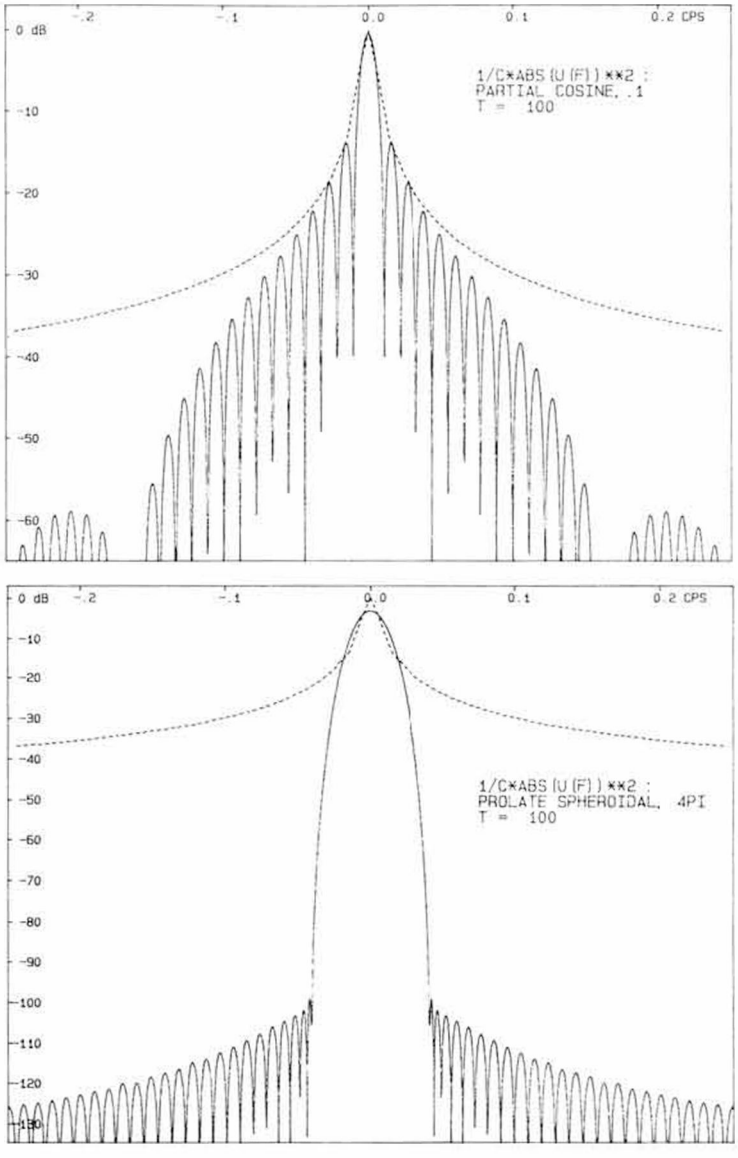

Fig. 2. Squared frequency window of the *partial cosine* taper (d = 0.1) and of a *prolate spheroidal* taper. For the latter notice the width of the main lobe and the very fast decrease of the side lobes.

of the spectral density difficult. A better estimate of the spectral density can be obtained by smoothing the raw periodogram (tapered or untapered). A weighted average of the form

$$\hat{S}_{xx}(f) = 1/CW \sum_{k=-K}^{k=K} W(k/K)\, I_{xx}(f - k\Delta f) \text{ with } CW = \sum_{k=-K}^{k=K} W(k/K) \quad (14)$$

is often used, where $W(x)$, $-1 < x < 1$, is a further window (sometimes called the spectral window) and K a user-chosen window width. It turns out that the quality of the estimate $\hat{S}_{xx}$ does not depend strongly on the actual shape of the spectral window but rather only on its bandwidth. The bandwidth is related to the concept of equivalent number of degrees of freedom which describes the asymptotic distribution of the estimate. For finite data, however, tapering increases the variability of the estimates, while, by its very purpose, it decreases the bias. There is a trade-off between low bias and low variance, both being not achievable simultaneously. Because both bias and variance also depend on the unknown spectral density, there is no spectral window or taper superior to all others in every situation.

An alternative way of producing an estimate with a smaller variance consists in averaging the periodogram values for K (K plays the role of the bandwidth of the above spectral window) different, possibly overlapping segments of the series [Welch, 1967]. Welch's approach has two advantages: (1) it allows some testing of the sta-

tionarity of the process under study, and (2) it permits an internal (i.e. obtained from the data) estimation of the variability of the periodogram. It has the disadvantage of increasing the leakage for a given total amount of data (see figure 1).

Apart from statistical considerations, segmentation and averaging may be preferred for pure technical reasons, as the order of the Fourier transform and the memory buffer size are smaller than in the case of Fourier transforming the data segment first and averaging over frequency afterwards. This can be crucial in the case of on-line multichannel data processing.

Distributional Properties

Individual periodogram values are asymptotically distributed as $S_{xx}(f)/2$ times a chi-squared variable with 2 d.f. for f not equal 0 or f_{Ny}.

The asymptotic distribution of the smoothed periodogram S_{xx} as in equation (14) is that of a weighted sum of chi-squared variables with 2 d.f. This distribution is usually approximated by that of a multiple of a chi-square variable with, say, E degrees of freedom. E is called the *equivalent number of degrees of freedom* and depends on the window used. This approximation can be used in a straightforward manner to set up confidence intervals for the spectral density. A logarithmic transformation of the spectral estimates tends to produce a better approximation to the normal distribution and also a frequency-independent asymptotic variance.

Confidence intervals for the coherence can be obtained by recalling that the coherence can be interpreted as the correlation of the components of the two processes at a specified frequency. This suggests using Fisher z-transform to obtain approximate, frequency-independent, confidence intervals. Not much is apparently known about the quality of these approximations. For problems and pitfalls in connection with the use of coherences in the EEG domain see French and Beaumont [1984].

Prewhitening

Problems of leakage, i.e. bias of the spectral estimates in the neighborhood of peaks, can be alleviated to some extent by the use of sophisticated tapers. If the expected range of the spectrum of interest varies over several orders of magnitude, a not too uncommon situation in many fields, including, occasionally, EEG, a better solution, particularly with short records, and also in view of the smoothing usually applied to the raw periodogram, is to be seen in the technique of prewhitening (also called prefiltering). This consists in transforming the data by a linear filter which cuts off the highest peaks (or troughs) from the spectrum. The spectrum, of reduced range, of the transformed data is then estimated in the way previously described and afterwards transformed back to the original coordinates using standard properties of the transfer function of linear filters. A simple way of designing such a filter consists in fitting an autoregressive process of low order to the data [see e.g. Kleiner et al., 1979].

Computational Procedures

Computation of power spectra and coherences is now straightforward: The basic estimate (Eq. 8) can be quickly computed at the Fourier frequencies $f_k = k/(N\Delta t)$, $k = 1, ..., N-1$ using the classical fast Fourier transform algorithm of Cooley and Tukey [1965] whose importance cannot be overestimated and which actually first made routine EEG spectral analysis realistic [Dumermuth and Flühler 1967]. Complete code for spectral estimation is nowaday available in many software packages. Therefore, we summarize here the basic steps from the data to the spectral density estimates including coherence for those users who have to build up programs, possibly tailored to special needs from more elementary pieces.

Some of these steps may not be required in many EEG analyses, while an on-line processing in the EEG laboratory may require additional steps for data acquisition, artifact control, A/D conversion, segmentation, etc. [see Dumermuth and Dinkelmann 1979]. Let then x[n], $n = 0, ..., N-1$ be a segment of N equispaced measurements provided by the A/D converter:

Step 1: The data are tapered giving $y[n] = u(n+0.5)/N)x[n]$. If the tapering is performed on the Fourier transform, which may be more efficient, this step is omitted.

Step 2: The tapered data are submitted to the fast Fourier transform. As a result the cosine and sine terms A[k] and B[k] at the Fourier frequencies $k/(N\Delta t)$, $k = 1, ..., N/2$ are obtained. N is usually a power of 2.

Step 3: The periodogram I_{xx} is obtained by squaring the absolute value of the complex Fourier transform or, equivalently, forming

$$I_{xx}[k/(N\Delta t)] = (A[k]^2 + B[k]^2)\, N\Delta t/4/C. \quad (15)$$

Recall that the periodogram is not changed for nonzero Fourier frequencies, whether or not the sample average is removed from the data before Fourier transforming. In the case where a second series y[n], $n = 0, ..., N-1$ is observed simultaneously, the cross-periodogram is cal-

culated similarly by multiplying the transform of one series by the complex conjugate of the transform of the other.

Step 4: More stable estimates $\hat{S}_{xx}$, $\hat{S}_{yy}$, $\hat{S}_{xy}$ are obtained by smoothing the (cross) periodograms according to equation (14). The amplitude and the phase spectrum can now be formed by taking the absolute value and the argument of $\hat{S}_{xy}$. Also transfer functions can be calculated. But of main interest is the coherence spectrum

$$\hat{\gamma}^2_{xy}[k/(N\Delta t)] = |\hat{S}_{xy}(k/N\Delta t)|^2/\hat{S}_{xx}(k/N\Delta t)/\hat{S}_{yy}(k/N\Delta t). \quad (16)$$

Note that a meaningless coherence of 1 is obtained if the calculation is performed before smoothing the periodogram!

Scaling of Power Density Spectra

The basic computations involve unscaled data which are only meaningful for normalized power density spectra or for coherence values. In the case of quantitative applications, where also comparability of the measurements is wanted, appropriate scaling of the power spectra is necessary.

The following parameters enter the scaling formula: G = total gain of all amplifier and filter stages; D = digital ADC output value corresponding to an analog input value of 1 V; C = taper or frequency window factor (e.g. 8/3 for a full cosine taper or hanning), and F = fast Fourier transform parameter (e.g. automatic scaling factor, π). A *power factor P* can be derived as follows:

$$P = 2FC[10^6/(GD)]^2. \quad (17)$$

The variance (power) s^2 of the EEG signal, expressed in μV^2, is equivalent to the integrated spectral density from the fundamental frequency 1/T to the Nyquist frequency f_{Ny}.

The scale of the spectral density is in μV^2/Hz or μV^2s. This means that e.g. in the case of white noise, the power value on the spectral plot has to be multiplied by f_{Ny} to obtain the total power or variance or, by taking its square root, the RMS amplitude (or standard deviation) in microvolts.

It is often convenient to display the power spectral density by its logarithm to the basis of 10 on a dB scale: power relations of 0.01, 0.1, 1, 10, 100, 1,000, and 10,000 correspond to dB values of −20, −10, 0, 10, 20, 30, and 40, etc. Using the power factor *P* defined above, the dB scale may be adjusted such that zero dB corresponds to 1 μV^2 of the EEG signal.

Length of Data Sample

A recurrent question is: how long a record should be used? It will be seen that no definite general answer to this question is provided here: moreover, even for well-defined problems the effective calculation of the required sample size involves a good deal of work and leaves one with a remarkable degree of uncertainty.

The reasons for this, actually not uncommon, situation can be outlined as follows. From an abstract statistical point of view, the requirements, in terms of stability and bias and/or resolution, of the estimates to be computed for the problem at hand should be first formulated; then, when worked out in detail, the asymptotics given by Dumermuth and Molinari [1986] provide (possibly after a preliminary study to determine data-dependent parameters of the estimation procedure, and if the necessary care has been used, e.g. to avoid artifacts) an approximation of the required record length. However, the quality of this approximation will generally remain unknown, depending in fact on higher order properties of the data.

From a more realistic point of view, sample sizes elaborated as just described are likely to come in conflict with our expectation about the range of stationarity of the EEG. In this case we see no way out of this conflict: Either we accept an increased variability or a reduced resolution of the estimates or a probable smearing over frequency of features of interest. Again a quantitative evaluation of this compromise is hardly feasible.

On Assumptions in Spectral Analysis

Stationarity

Stationarity is necessary in order that the computed quantities be estimates of well-defined parameters and not averages over time. Stationarity will seldomly be exactly satisfied in practice, but often approximately if the time span ot the series is short enough, so that the parameters of interest do not change too much during the epoch.

Well-known examples of nonstationarities in the EEG are the sleep cycles, where changes in total power, shifts of power between frequency bands, and even a time-dependent coherence structure can be observed (see figure 7) [Dumermuth et al., 1983b]. Nonstationarities may further be due to changes in vigilance level, performing of tasks, effects of drugs, etc.

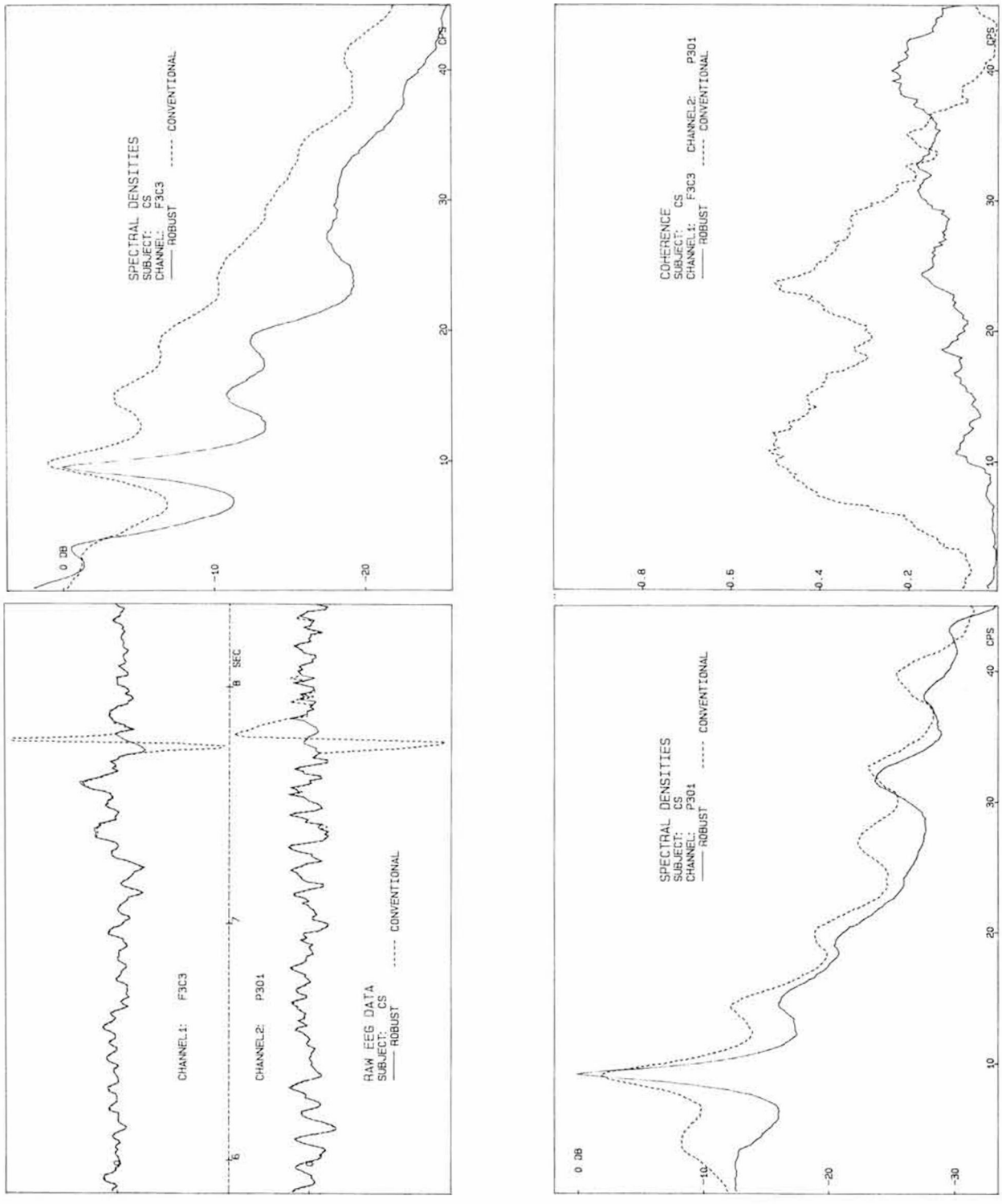

Fig. 3. Conventional and robust spectral analysis of an EEG segment with artifacts. A segment of 10 s EEG (sampling rate 102.4/s, analog low-pass filter at approximately 40 Hz) from bipolar derivations F3C3 and P301 has been submitted to spectral analysis. The data include artifacts due to electrical contamination. The figure shows first part of the original (dotted line) and 'robustified' (continuous line) raw data for both channels. Amplitudes are on an arbitrary scale. Following the raw data the conventional and robust estimated spectral densities are shown. The data have been previously prewhitened by fitting an AR process of low order, then a partial cosine taper (d = 0.1) has been applied. The periodogram has been smoothed by a simple moving average of half size of 50 and eventually recolored. Finally the conventional and robust coherence of the two derivations are given.

Ergodicity and Mixing

Ergodic processes have the property that ensemble averages of functions of the observations are equal to the corresponding time averages. In most practical cases, including most aspects of EEG, we do not have repeated realizations available, and, therefore, we cannot really check this assumption. This is the case for spontaneous ongoing EEG, where the ensemble consists of all conceivable EEGs for the subject at hand in the present situation, but just one EEG can be recorded. In order that the usual estimates of the spectral density have decent statistical properties, we require stronger assumptions on the process than ergodicity, namely some kind of mixing (mixing assumptions relate to the span of dependence of the process and imply that this is short enough). In this sense ergodicity is not a crucial requirement.

Normality

Spectral analysis based on Fourier transforming the time series is nonparametric, and, insofar, a normality assumption is not required. While normal or Gaussian processes are completely described by the mean and the autocovariance function (2nd-order moment) or, equivalently, by the spectral density, non-Gaussian processes require, for a more complete description, the study of higher-order moments. Deviations from normality in the EEG are of interest because of their implications with regard to its generating mechanisms: of special interest are dependencies among frequency bands which are not detectable by spectral analysis alone, but require at least the study of the bispectrum.

A particular type of nonnormality occurs when the observed process can be looked at as the sum of a Gaussian process of interest and of a corrupting process, consisting of artifacts, or outliers, of any kind. Assuming the corrupting process can be modeled as a stationary process too, then the standard asymptotics will work, and we will be estimating the spectral density of the sum process. But this is not the goal of the analysis. Rather we want to study the underlying process and discard, or isolate, as far as possible, the artifacts.

The corrupting process can distort the spectral density of interest in a variety of ways. This is true even in the case of corrupting white noise, as soon as its power is not negligible with respect to the spectral density under study and is especially relevant if the corrupting process contains strong rhythmic components: in this case the form of the spectrum can be radically changed.

Also, isolated (not necessarily large) outliers induce an oscillating behavior into the periodogram which may completely obscure the features of interest. Therefore, safeguarding against outliers is particularly important when the analysis, or parts of it, is done automatically. To deal with this problem, so-called robust methods for spectral analysis have been recently suggested (next section).

Robustness in Spectral Analysis

Robustness is a property of statistical procedures (estimators and tests) which makes them insensitive to small deviations from the assumptions for which their properties exactly hold.

A general paradigm for robust data analysis has been formulated by Huber in the discussion of Kleiner et al. [1979]. Within this scheme the analysis of interest is applied not to the original data but to a set of cleaned data, where cleaning essentially means downweighting (down to rejection) isolated data points which do not fit a postulated model.

The procedure described in Kleiner et al. [1979] is fairly effective and easily implemented. It consists in applying the routine procedure for spectral analysis, with the steps of tapering, Fourier transforming, squaring and smoothing, not to the original data, but rather to 'robustified' residuals from robustly fitting an autoregressive process of low order to the original data.

The actual spectral density of interest is then obtained by transforming back as in conventional prewhitening. We give here an example (fig. 3) of applying this procedure to two channels of EEG data, where some emphasis is on the robust estimation of coherence. Additional examples as well as more detailed considerations about robustness in time series are given in Molinari and Dumermuth [1986].

Postprocessing of Spectral Data

Merely Fourier transforming EEG data does not yield any data reduction: in fact the original data can be fully recovered by the inverse transform. Although calculating smoothed spectral densities represents a first step toward data reduction, the amount of data produced by spectral analysis of a long, possibly nonstationary segment of multichannel EEG is still very large and calls vehemently for further steps of condensation, parameter extraction, suitable synopsis, and statistical treatment.

Many techniques have been suggested to perform these steps, a number of them being listed in table I. As it would be hopeless to give an exhaustive critical account

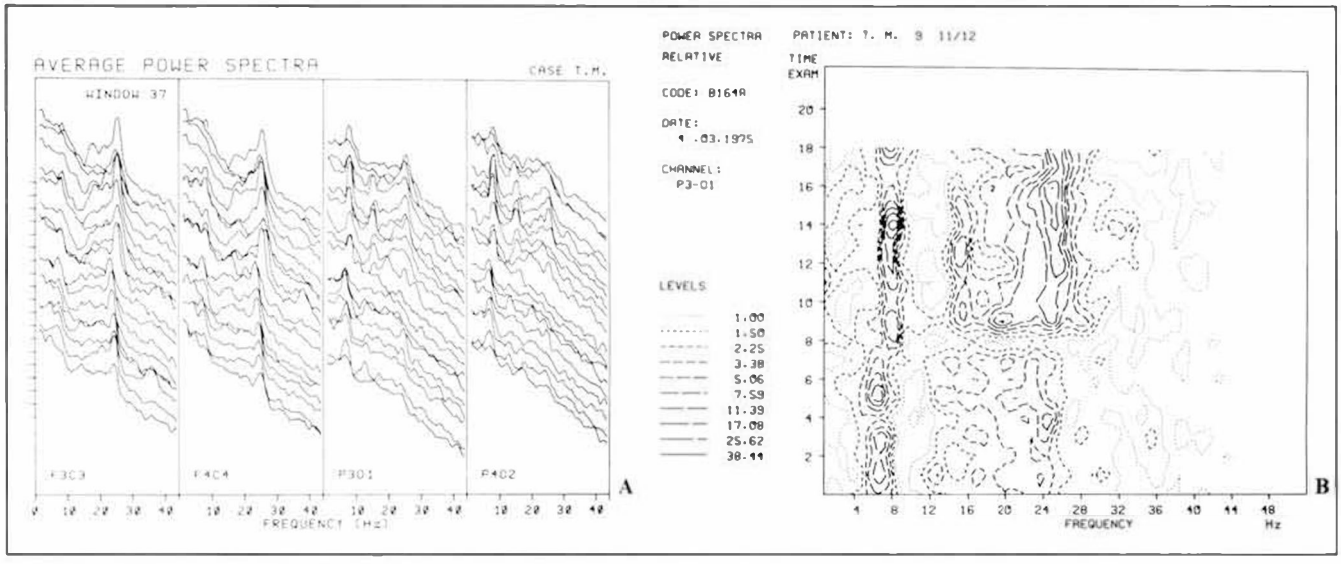

Fig. 4. Sequential spectral displays and contour plot of EEG power spectra series. Average power spectra measured from 19 EEG recordings during a 1-year observation epoch [from Dumermuth, 1977]. **A** Sequential power spectrogram: pronounced alpha and beta activity is observed in all samples. The first nine spectra (bottom to top) were recorded while the patient was under mixed medication with clonazepam, DPH, and primidone, the subsequent series during clonazepam monotherapy, with exception of the last which was recorded under jodazepam monotherapy. Note the marked differences in alpha and beta activity during the two series and a further change in beta activity in the anterior derivations of the last sample (top left side). After change of medication (observations 10–19) the clinical condition was drastically improved. **B** Countour plot of channel P3-01: the peak frequency shifts and peak power increase in alpha and beta activity due to changed medication are displayed in a still dynamic but more quantitative way than in **A**.

Table I. Postprocessing of spectral data

Parameter extraction
Band power, band coherence
Power of white, pink, and colored noise components
Baseline slope and intercept
Peak parameters (see table II)
Spectral quotients
Condensation and synoptic presentation
Sequential spectral or coherence displays
Compressed spectral arrays
Contour plots
Topographic parameter displays
Three-dimensional scalp maps
Chernoff faces
Statistical Treatment
Simple treatment
Mean and standard deviation of spectral parameters
Average spectra with range of variance
Product-moment correlation of power spectra
Analysis of variance
Multivariate analysis
Principal component and factor analysis
Multidimensional scaling
Multivariate analysis of variance
Discriminant analysis
Cluster analysis
Nonlinear pattern classification

of most of them, we will limit this important topic to a few examples and some considerations of a general nature and selected references.

Condensation

Condensation into plots of consecutive power or coherence spectra such as serial spectrograms, compressed spectral arrays, sequential spectral power or coherence displays, or contour plots allows a direct visual assessment of relatively large amounts of spectral data. Such condensed displays indicate temporal variability as well as the time when events or marked changes occur (fig. 4).

Parameter Extraction

Automatic extraction of spectral parameters is probably the most important way to process spectral output economically. Ad hoc parameters may be defined either on the basis of physiological and clinical considerations or in the effort of reproducing the descriptive criteria used in visual evaluation of the EEG, or both. One way is to define frequency bands, either in equal steps or following the classical frequency bands delta, theta, alpha, and beta. In the latter case, however, difficulties may arise with spectral peaks at band boundaries, as e.g. between theta and alpha in small children. Plotting band power and band coherence against time has shown to be

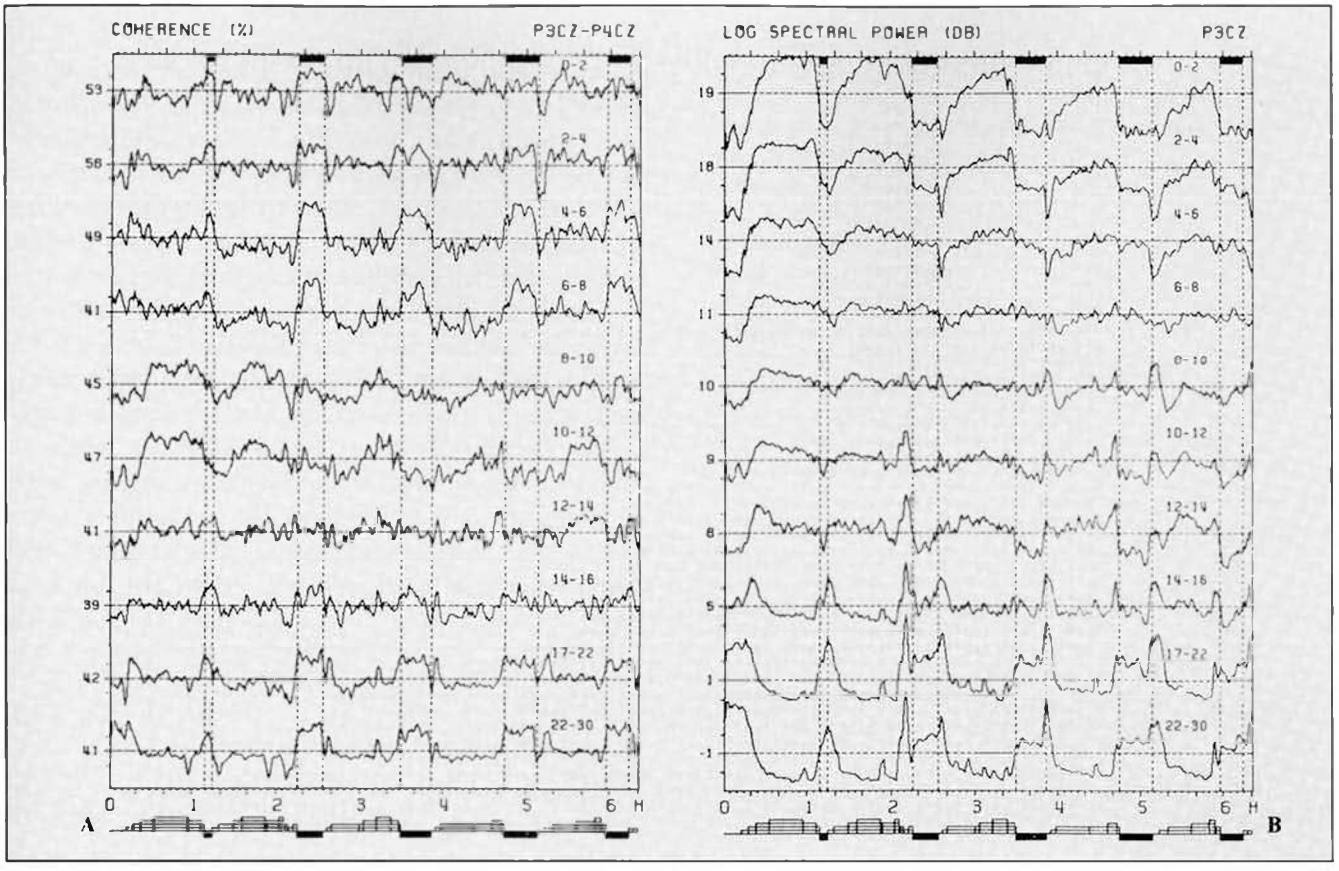

Fig. 5. Temporal profiles of spectral band power and band coherence. Example of spectral analysis of all-night sleep EEG in 10 frequency bands [from Dumermuth et al. 1983b]. At bottom of each plot sleep stages 1–4, REM and waking state (no elevation) are indicated. The black bars together with the dashed vertical lines mark REM sleep periods. Frequency bands are indicated at right. **A** Spectral power: the left parietal to vertex derivation is displayed on a logarithmic scale. The numbers on the left side represent mean power in dB, the small marks indicate ± 3 dB. Notice the pronounced sleep stage dependent power changes, especially in the slow and fast frequency bands, as well as the decreasing power maxima from cycle to cycle at the slow frequencies. **B** Coherence: display of interhemispheric coherence between parietal to vertex derivation (the numbers on the left side represent mean coherence in percent, the small marks indicate ± 10%). Note the characteristic changes of coherence, dependent on sleep stage, frequency, and derivation. Especially pronounced are the increases during REM in the slow and fast frequency bands.

extremely illustrative to characterize the temporal dynamics of long-term recordings, as e.g. in all-night sleep (fig. 5).

Another approach is to first divide the power spectrum into three major components, i.e. (1) a *flat white noise* part, (2) a *pink noise* part, with gradually decaying power from the slow to the fast end of the EEG spectrum, and (3) a *colored noise* part representing the power of the peaks. The power spectrum may now be regarded as a superposition of the three independent components.

The white noise part is not generally of much interest. In most cases, where it contributes significantly to the total power, it may indicate technical or biological artifacts or pronounced outliers in the EEG itself like irregular series of epileptic spikes.

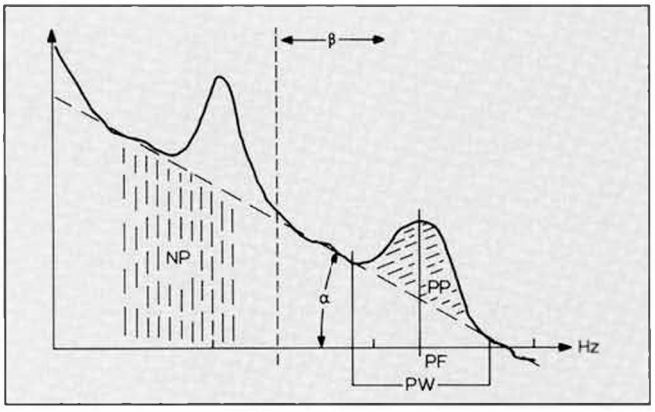

Fig. 6. Extraction of spectral parameters in power spectra: NP = Noise power; PP = peak power; PF = peak frequency; PW = peak width; SL = baseline slope = tan (a), see also table II. [From a study on beta activity by Dumermuth et al. 1983a.]

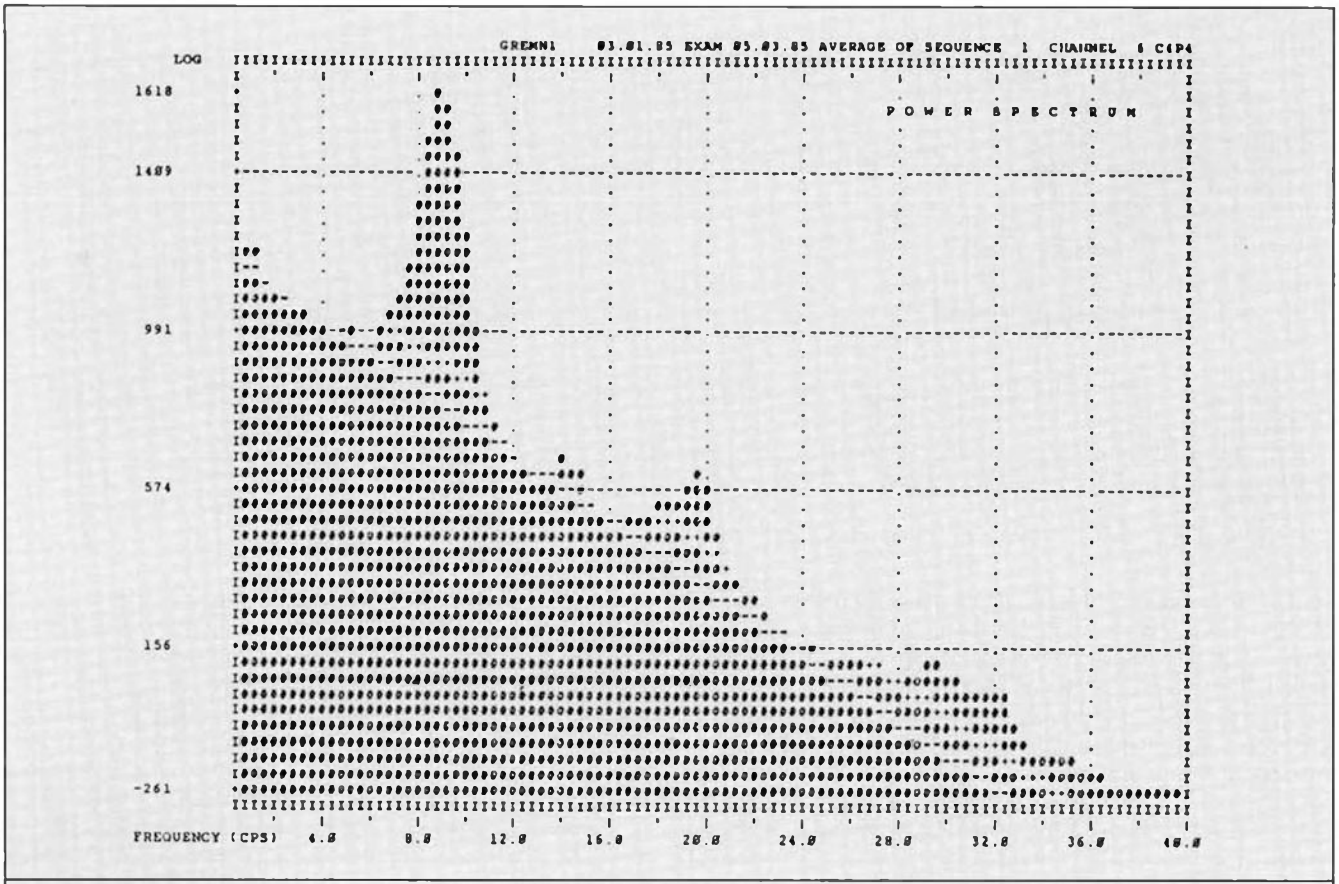

7A

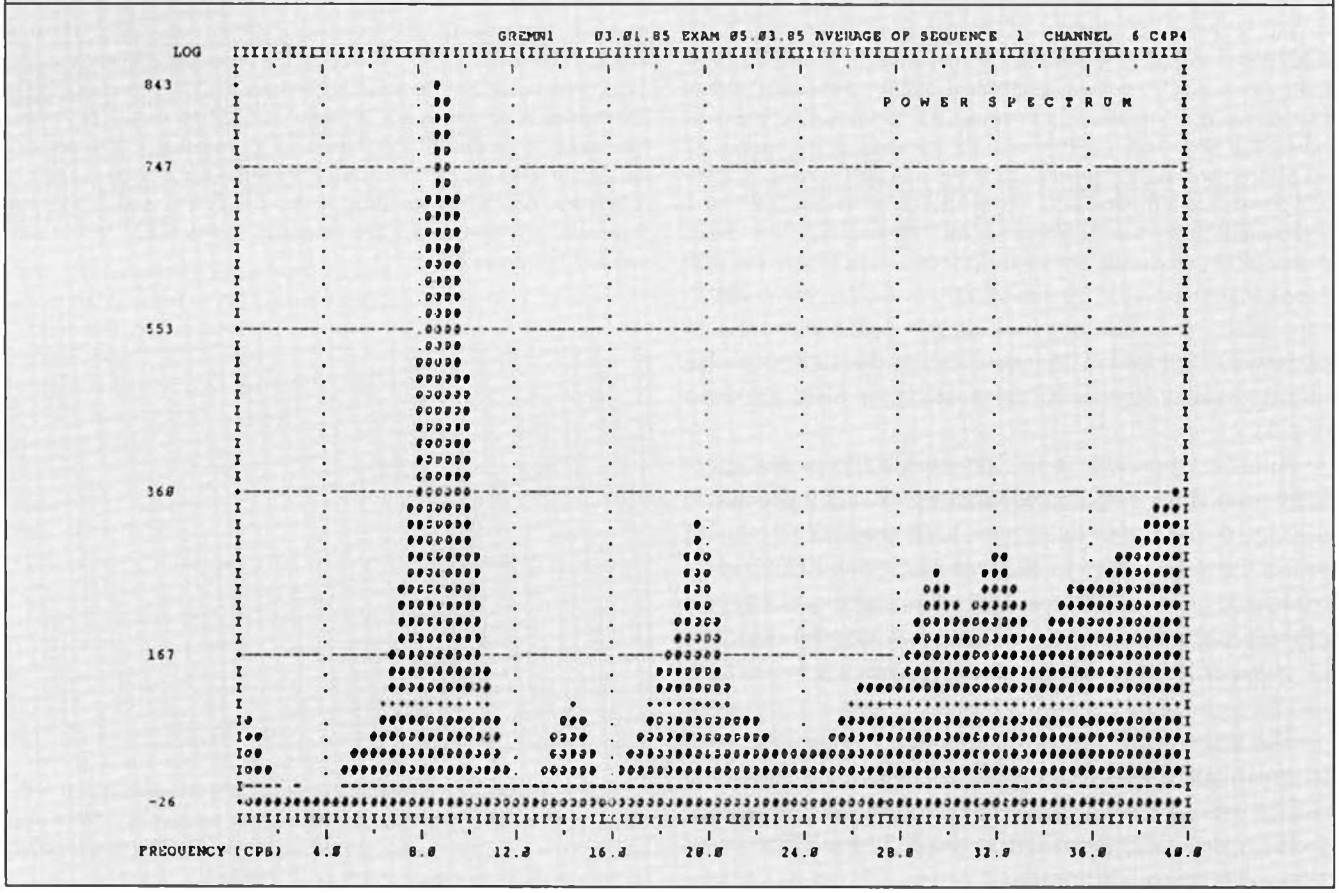

7B

Of more interest is the pink noise component: in actual observations its spectral shape very often follows a decaying exponential function or a straight line in log representations which can be characterized by the slope parameter tan α (fig. 6) and the intercept. The pink noise may be thought of as the underlying unstructured EEG component which is a natural feature of empirical data and often called *amorphous* or *arrhythmic activity.*

The most interesting part is, of course, the colored noise component, represented by the particular power distribution in the form of one or several spectral peaks. As shown in figures 6 and 7A and in table II, various peak parameters may now be defined and extracted. Subtraction of the pink noise part from the spectrum before processing the peaks of the colored noise component is often quite useful and to be recommended (fig. 7B, C).

Table II. Spectral parameters

Power of white, pink, and colored noise components
Band power and band coherence
Baseline slope and intercept
Peak parameters
Peak frequency
Peak power (peak area)
Relative spectral peak power (%)
Halfpower bandwidth
Peak width (distance between peak footpoints)
Peak skewness (asymmetry coefficient)
Peak kurtosis (peak shape)
Spectral quotients
Hjorth parameters

This list is not exhaustive. Furthermore, the relative figures of merit of the parameters listed above are not fully assessed yet. See figure 6.

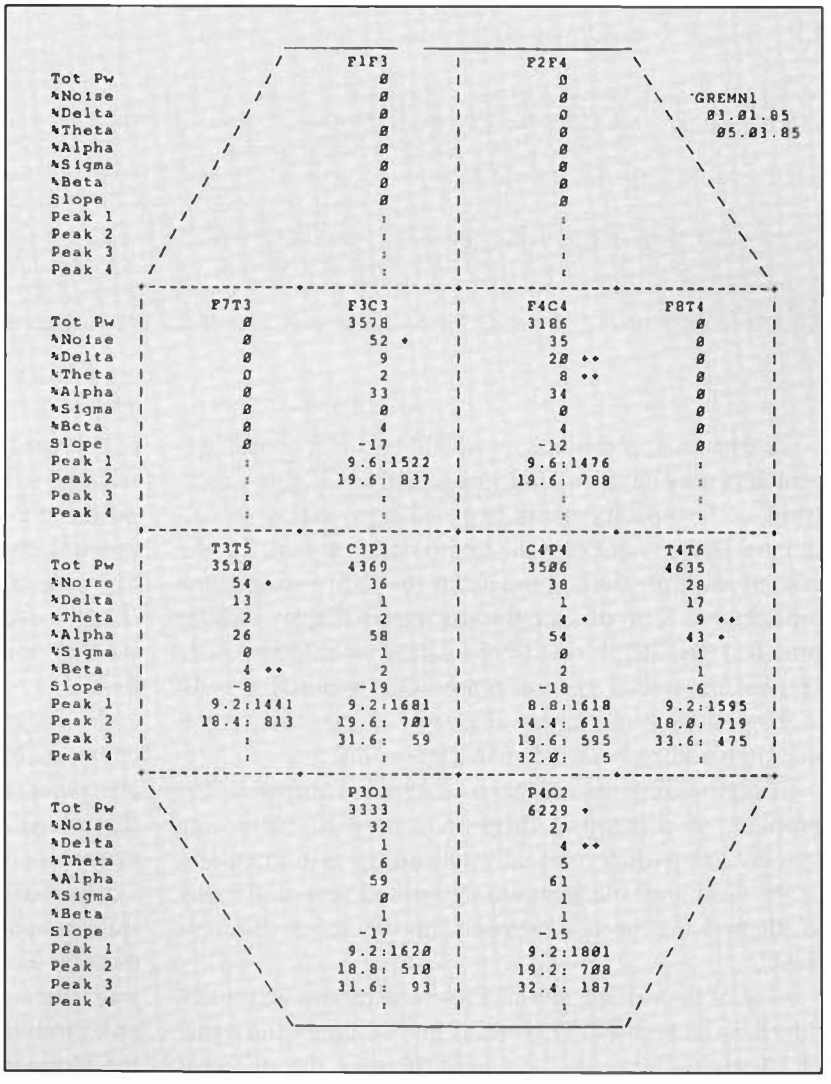

Fig. 7. On-line postprocessing of clinical routine EEG: On-site and on-line preprocessing of 8-channel EEG with PDP LSI-11 based microcomputer satellite system according to Dumermuth and Dinkelmann [1979]. On-line postprocessing by host computer (PDP11/34-55) produces serial plots of log power and coherence spectra. From averages over 14 consecutive segments of 20 s each – (illustrated for C4P4 before (**A**) and after (**B**) subtraction of pink noise part) – a topographical parameter display (**C**) is obtained (log power values are unscaled).

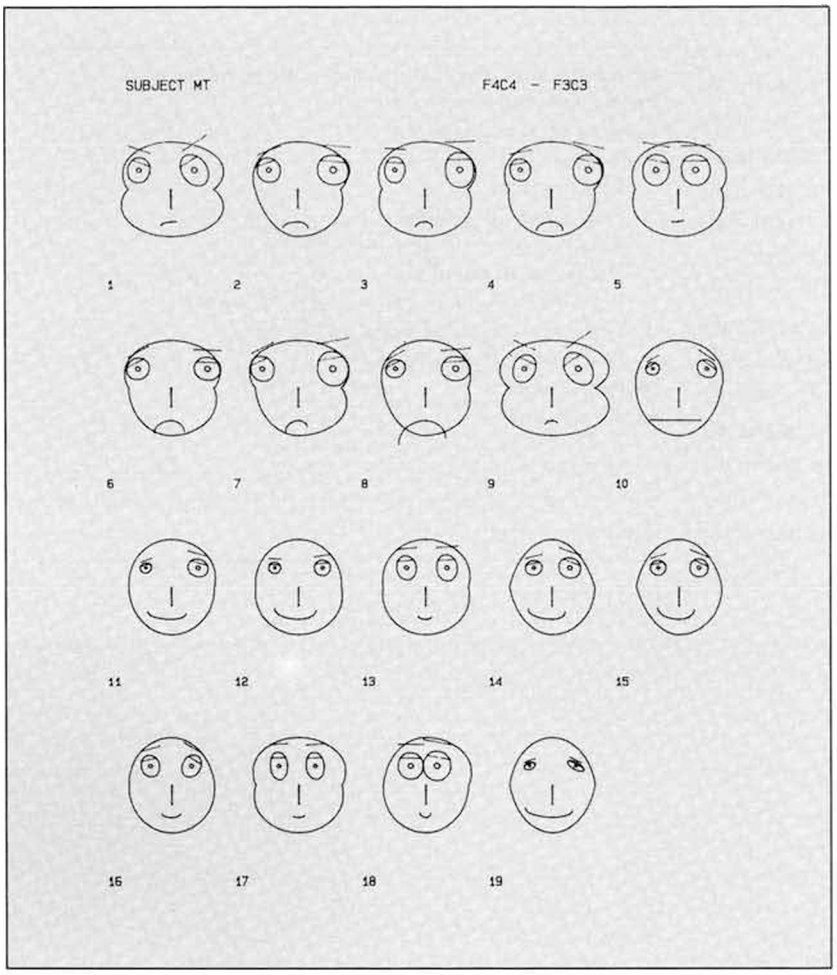

Fig. 8. Chernoff faces for 19 EEG spectra (same observations as in figure 6A). From the spectra ten parameters are extracted and transformed to the value of certain face parameters (other face parameters are kept constant). The left side of the face corresponds to the derivation F4C4, the right side to F3C3. Note impressive change in facial expression after change of therapeutic regimen (faces 10ff.).

In certain applications quotients between certain parameters may be calculated, either within the same spectrum or for spectral pairs (e.g. left-right ratios of delta/beta power quotients in homologous areas). In the case of multiple derivations from the entire scalp some topographic form of synoptic parameter display may be practical (fig. 7C). Using interpolating techniques, topographic parameter mapping provides impressive well-looking three-dimensional displays of the data, serial mapping adding even a fourth dimension.

If highly dimensional parameters are computed, the problem of presenting them in a way to make one quickly grasp their mutual relationship is particularly acute. Graphical methods are well suited here, and many of them have been developed in the most different fields.

One of the earliest among these techniques was introduced by Chernoff [1973] and is known under the name of Chernoff faces. In the Chernoff faces the different components of the original data vector are made to correspond to features of faces (e.g. eye and mouth location, height of nose, etc.); in this way each highly dimensional spectral data point corresponds to a face, where the human eye can assess essential similarities or dissimilarities (or even find clusters) between faces better and faster than a numerical algorithm working on the original data.

If – in contrast to the original idea of Chernoff – we construct both sides of the face with homologous parameter pairs, these faces become well suited to the EEG in that its symmetry (or asymmetry) is now reflected in the symmetry (or asymmetry) of the face. However, one difficulty with the Chernoff faces lies in the relatively arbitrary assignment of face parameters to the original coordinates. This choice may influence, in an unpredictable way, the visual assessment of the faces. Figure 8 shows an example of Chernoff faces [for another EEG example see Molinari and Dumermuth 1983].

References

Bingham, C.; Godfrey, M.D.; Tukey, J.W.: Modern techniques of power spectrum estimation. IEEE Trans. Audio-Electroacoust. *AU-15:* 56–66 (1967).

Chernoff, H.: Using faces to represent points in K-dimensional space graphically. J. Am. statist. Ass. *68:* 361–368 (1973).

Cooley, W.J.; Tukey, J.W.: An algorithm for the machine calculation of complex Fourier series. Maths Comput. *19:* 297–301 (1965).

Dumermuth, G.: Fundamentals of spectral analysis in electroencephalography; in Remond, EEG-informatics. A didactic review of methods and applications of EEG data processing (Elsevier/North Holland, Amsterdam 1977).

Dumermuth, G.; Dinkelmann, R.: EEG data acquisition and preprocessing by microcomputer satellite system. Comput. Programs Biomed. *10:* 197–208 (1979).

Dumermuth, G.; Flühler, H.: Some modern aspects in numerical spectrum analysis of multichannel electroencephalographic data. Med. biol. Eng *5:* 319–331 (1967).

Dumermuth, G.; Lange, B.; Herdan, M.: Analyse spectrale de l'activité EEG rapide (bêta). Rev. Electroencéphalogr. Neurophysiol. *13:* 122–128 (1983a).

Dumermuth, G.; Lange, B.; Lehmann, D.; Meier, C.A.; Dinkelmann, R.; Molinari, L.: Spectral analysis of all-night sleep EEG in healthy adults. Eur. Neurol. *22:* 322–339 (1983b).

Dumermuth, G.; Molinari, L.: Spectral analysis of EEG background activity; in Gevins, EEG handbook, (in press, 1987).

French, C.C.; Beaumont, J.G.: A critical review of EEG coherence studies of hemisphere function. Int. J. Psychol. *1:* 241–254 (1984).

Harris, F.J.: On the use of windows for harmonic analysis with the discrete Fourier transform. Proc. IEEE *66:* 51–83 (1978).

Kleiner, B.; Martin, R.D.; Thomson, D.J.: Robust estimation of power spectra. J.R. statist. Soc. *B41:* 313–351 (1979).

Molinari, L.; Dumermuth, G.: Analyse multivariée de l'activité bêta dans un matériel clinique. Rev. Electroencéphalogr. Neurophysiol. *13:* 129–136 (1983).

Molinari L.; Dumermuth, G.: Robust spectral analysis of the EEG. Neuropsychobiology *15:* 208–218 (1986).

Thomson, D.J.: Spectrum estimation techniques for characterisation and development of WT4 waveguides. I and II. Bell Syst. Tech. J. *56:* 1763–1815; 1923–2005 (1977).

Van Schooneveld, C.; Frijling, D.J.: Spectral analysis: on the usefulness of linear tapering for leakage suppression. IEEE Trans. Acoust. Speech Signal Process. *ASSP-29:* 323–329 (1981).

Welch, P.D.: The use of fast Fourier transform for the estimation of power spectra: a method based on time-averaging over short modified periodograms. IEEE Trans. Audio-Electroacoust. *AU-15:* 70–73 (1967).

Further Reading

Blackman, R.B.; Tukey, J.W.: The measurement of power spectra from the point of view of communications engineering (Dover, New York 1958).

Brigham, E.O.: The fast Fourier transform (Prentice Hall, Englewood Cliffs 1974).

Brillinger, D.R.: Time series: data analysis and theory (expanded ed. Holden Day, San Francisco 1981).

Chambers, J.M.; Cleveland, W.S.; Kleiner, B.; Tukey, P.A.: Graphical methods for data analysis. (Duxbury Press, Boston 1983).

Durrani, T.S.: Special issue on spectral analysis. Proc. IEE *130 F:* 193–288 (1983).

Gevins, A.S.: Analysis of the electromagnetic signals of the human brain: milestones, obstacles and goals. IEEE Trans. biomed. Engng *BME-31:* 833–850 (1984).

Haykin, S.; Cadzow, J.A.: Special issue on spectral estimation. Proc. IEEE *70:* 881–1136 (1982).

Priestley, M.B.: Spectral analysis of time series, vols 1 and 2 (Academic Press, London 1981).

Prof. G. Dumermuth,
Universitäts-Kinderklinik,
Steinwiesstrasse 75,
CH–8032 Zürich (Switzerland)